



Omnidirectional Multi-lobe Passive Direction Finder with Modified Butler Matrix Algorithm Using

E. Hosko* and J. Vesely

Department of Radar Technology, University of Defence, Brno, Czech Republic

The manuscript was received on 10 June 2010 and was accepted after revision for publication on 14 September 2010

Abstract:

The article deals with an omnidirectional multi-lobe passive direction finder (PDF) that uses the modified Butler matrix operation algorithm and a digital amplitude direction finding method for the direction of arrival determination of the signal of interest. The article brings a concept of the PDF with the multi-lobe circular antenna array (CAA) for the omnidirectional interception of signals and results of the DOA determination obtained with the experimental CAA. These practical results of measuring with experimental CAA are compared with the theoretical results obtained by means of mathematical models of the PDF based on an approximation of real antenna patterns. To approximate the real antenna pattern of CAA antenna elements, an appropriate form of the Gaussian curve is used.

Keywords:

Digital amplitude direction finding method, direction of arrival determination, modified Butler matrix operation algorithm, multi-lobe circular antenna array, omnidirectional direction finding

1. Introduction

The current situation in radar signal sources area is characterized by a permanently significant growth of LPI (Low Probability of Intercept) radars. Generally, this complex situation makes difficult conditions for electronic intelligence (ELINT) and the operation of passive surveillance systems (PSS) from the LPI radar signal interception point of view. This situation is typical for long-based multi-positional PSS using the time-difference-of-arrival (TDOA) method of signal sources location determination.

* Corresponding author: Department of Radar Technology, University of Defence, Kounicova 65, 662 10 Brno, Czech Republic, phone: +420 973 445 020, E-mail: eduard.hosko@unob.cz

One of possible solutions of the LPI signal interception problem is to use an antenna array that will cover the whole area of interesting (e.g., required angular sector) by its antenna pattern. In the case of a requirement to cover the whole azimuth plane, a possibility to use a circular antenna array (CAA) with multi-beam antenna pattern in the azimuth is offered. To improve receiving conditions, it is recommended to use antenna elements with an acceptable and sufficient directivity. To determine the emitter location, i.e. a direction of arrival (DOA) by a passive direction finding (DF) system with the CAA, it is possible to use a digital amplitude (DF) method. This method is based on the knowledge of the magnitude of receiving signal amplitudes yielded by relevant CAA elements and the operation algorithm of a modified Butler matrix (MBM) [1, 2].

The used digital amplitude DF method for the DOA determination is appropriately accurate as far as the used CAA has an adequate number of antenna elements and there are a sufficient number of received signals for DOA computing by using of the MBM operation algorithm. When the passive DF system cannot use an adequate number of received signals, the advantage of the digital DF method using is lost and the final emitter location determination accuracy is poor. However, in spite of the above mentioned circumstances, the direction finder with the amplitude DF method based on the MBM operation algorithm using offers more simple solution of its design and construction. Simultaneously, the DOA determination of signal sources by means of digital amplitude DF method can use all advantages of the amplitude based DF method compared to the other DF methods (e.g., phase interferometer method).

2. Concept of Passive Direction Finder with Multi-lobe Circular Antenna Array

For an omnidirectional DOA determination the main task of an omnidirectional PDF design is to ensure the signal interception from the whole azimuth plane or a required angle sector. Therefore an interconnecting network is used to connect all elements of an antenna array to signal processing circuits to receive the signal of interest and determine the DOA of signal sources. This interconnecting network is called the Beam Forming Network (BFN) because this circuitry of microwave elements enables to create multi-lobe antenna pattern covering an angle area of interest.

For the microwave region, there are two basic approaches to realize the BFN of a multi-lobe antenna array. The first one is so-called Blass matrix that consists of a set of travelling-wave feed lines connected to a linear array crossing another set of lines and directional couplers interconnecting the two sets of lines. The topology of the Blass matrix is such that beams are formed in different directions and the aperture illumination is defined by the coupling coefficients of the couplers [3].

The second one is known as the Butler matrix which consists of fixed phase shifts interconnected to hybrid couplers (hybrids) and yields orthogonal beams (they have usually -3.9 dB-beam crossovers). The introduction of 180-degree hybrids can significantly reduce the number of phase shifters. In addition, the minimum phase shift is twice that for a 90-degree hybrid matrix and this property facilitates the maximum matrix size constraint [3].

For the passive omnidirectional signal interception requirement at the whole azimuth plane the Butler matrix (BM) as the BFN is usually used because this type of the BFN ensures the fixed position antenna pattern beams and can use a circular

antenna array to cover the angle area of interest. On the other hand, the using of the BM means to make use of 2^N antenna elements and the corresponding number of hybrids at the matrix topology. Next, the N defines the total losses rising from a signal passing through used hybrids. For example, if the PDF consists of the four-element CAA, the BM will create 2 times 2 (2×2) hybrids to interconnect antenna elements to signal processing circuitry. Therefore N is equal to 2. It means that each signal intercepted by an antenna element will be attenuated by -6 dB at output ports of the BM. In the case of eight-element CAA using ($8 = 2^3$), the total losses of intercepted signals will be -9 dB at the BM output ports and so on.

2.1. Passive Circular Interferometer Direction Finder

Fig. 1 is a block diagram of the four-element interferometer bearing discriminator and is presented to show a typical passive circular interferometer direction finder [4]. This DF system uses four (typically broadband) antennas directed to the north, the east, etc. to cover 360 degrees in the azimuth plane and to determine the DOA of incoming signals.

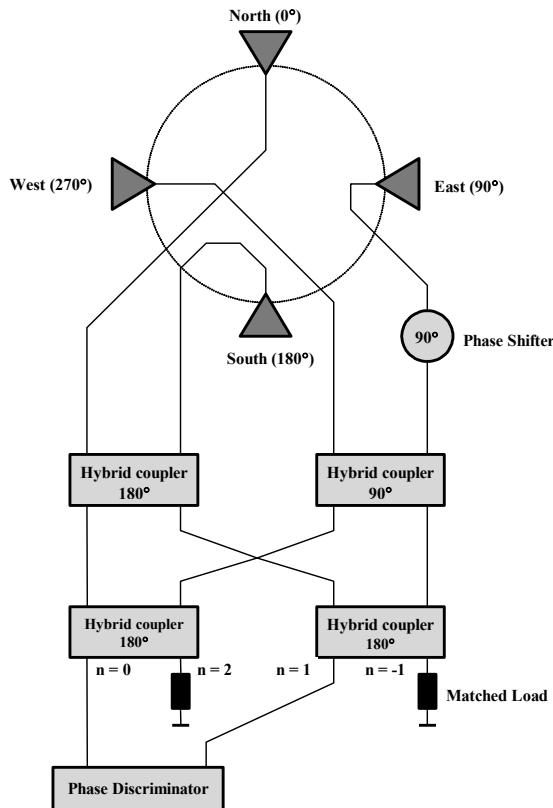


Fig. 1 The block diagram of an interferometer bearing discriminator with four-element Butler-fed circular array [4]

For the DOA determination of signals of interest there are compared the bearing angles at the output port $n = 0$ to $n = 1$ of the strongest signal intercepted by elements of the CAA and the phase output will equal the phase input for 1:1 correspondence. Any signal appearing in between the antenna elements will interpolate [4].

Tab. 1 shows the results of additional phase shifts at the BM output ports for all signals intercepted by antenna elements of the CAA. These phase shifts are caused by passing signals through the phase shifter and hybrids used at the BM topology. From the values introduced in Tab. 1 it is evident that the signal from each antenna coming to the output port $n = 0$ has the total additional phase shift equal to 0. The signal at the output port $n = 1$ has the value of the total additional phase shift equal to the azimuth – the bearing angle of the corresponding antenna that intercepts the given (incoming) signal.

Tab. 1 Corresponding phase relationships at output ports due to antenna inputs [4]

Antenna (Sector)	Angle (Azimuth) [deg]	Additional Phase Shifts at BM Output Ports [deg]				
		$n = 0$	$n = 1$	$n = 2$	$n = -1$	Δ $N = 1$ to 0
North	0	0	0	0	90	0
East	90	0	90	180	0	90
South	180	0	180	0	270	180
West	270	0	270	180	180	270

To improve the angle sector resolution between adjacent antennas it is necessary to increase the number of the antenna element of the CAA used for signal interception. However, the BM topology shown in Fig. 1 and used for the four-element passive circular interferometer direction finder is not suitable and it is unavoidable to change the basic philosophy of the BM design as a BFN for the omnidirectional multi-lobe CAA used by PDF. Therefore a concept of the modified BM has been introduced which enables to increase the number of antenna elements used for signal interception by a simple way.

2.2. Modified Butler Matrix Design

In order to allow an extension of the antenna elements number used for the CAA design and an enlargement of the BM, it is necessary to change the topology of the BM shown in Fig. 1. The different approach of the BM design is based on using of the 180-degree phase shift at BM output ports that will correspond to a spatial angle of an opposite antenna pair. In the case of the four-element CAA, the one of the 180-degree hybrid coupler (HC 180) will connect the north antenna (N) with the south antenna (S) and the next one will connect the east antenna (E) with the west antenna (W). To interconnect these two antenna pairs, the second pair of hybrid couplers, the 180-degree one and the 90-degree one is used. The topology of this MBM used for the four-element CAA design is shown in Fig. 2. The introduced MBM has the dimension 2×2 because this designed BFN uses 2×2 hybrids for connecting four elements of the CAA to the four output ports of the MBM.

Tab. 2 shows the results of additional phase shifts at the MBM output ports for all signals intercepted by relevant antenna elements of the CAA. By analogy to the

interferometer bearing discriminator shown in Fig. 1, these phase shifts are caused by passing signals through the corresponding hybrids used for the MBM topology. From the values introduced in Tab. 2 it is then evident that the signal from each antenna coming to the output port $n = 0$ has the total additional phase shift equal to 0. The signal at the output port $n = 1$ has the value of the total additional phase shift equal to the azimuth – the bearing angle of the corresponding antenna that intercepts the given (incoming) signal. It means the change of the MBM topology does not affect the operation algorithm of the used BFN from the additional phase shift point of view.

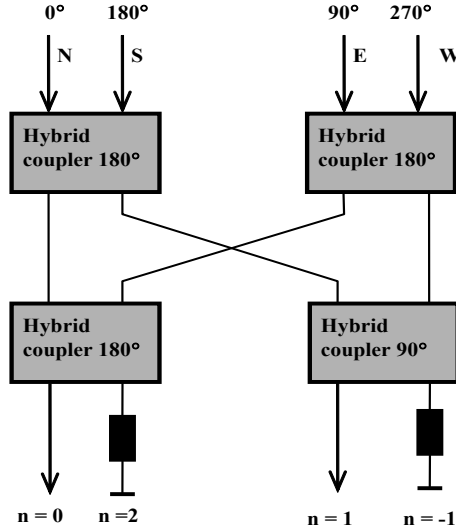


Fig. 2 The block diagram of modified Butler matrix for four-element CAA [2]

Above all, the topology of the MBM depicted in Fig. 2 is very convenient for the next enlargement of the MBM by a simple way. For example, to enlarge the MBM for feeding the eight-element CAA, it is realised by the two MBMs from Fig. 2 and their mutual interconnecting by the 180-degree hybrid in the third line. To obtain the 45-degree phase shift between outputs ports of this 2×2 MBM pair, a fixed-phase shifter with the 45-degree phase shift has been used. This method enables to enlarge the MBM for connecting 2^N CAA elements where N is 2, 3, 4, etc.

Tab. 2 Values of additional phase shifts of the MBM used to feed the interferometer bearing discriminator with four antennas [2]

Antenna (Sector)	DOA (Azimuth) [deg]	Additional Phase Shifts at BM Output Ports [deg]				
		$n = 0$	$n = 1$	$n = 2$	$n = -1$	Δ $N = 1$ to 0
North	0	0	0	0	90	0
East	90	0	90	180	0	90
South	180	0	180	0	270	180
West	270	0	270	180	180	270

The design of the MBM for feeding an eight-element CAA is shown in Fig. 3. The values of the corresponding additional phase shifts at the MBM output ports for intercepted signals by relevant antenna elements are introduced in Tab. 3. These additional phase shifts are obtained by a similar way as used for the 2x2 MBM.

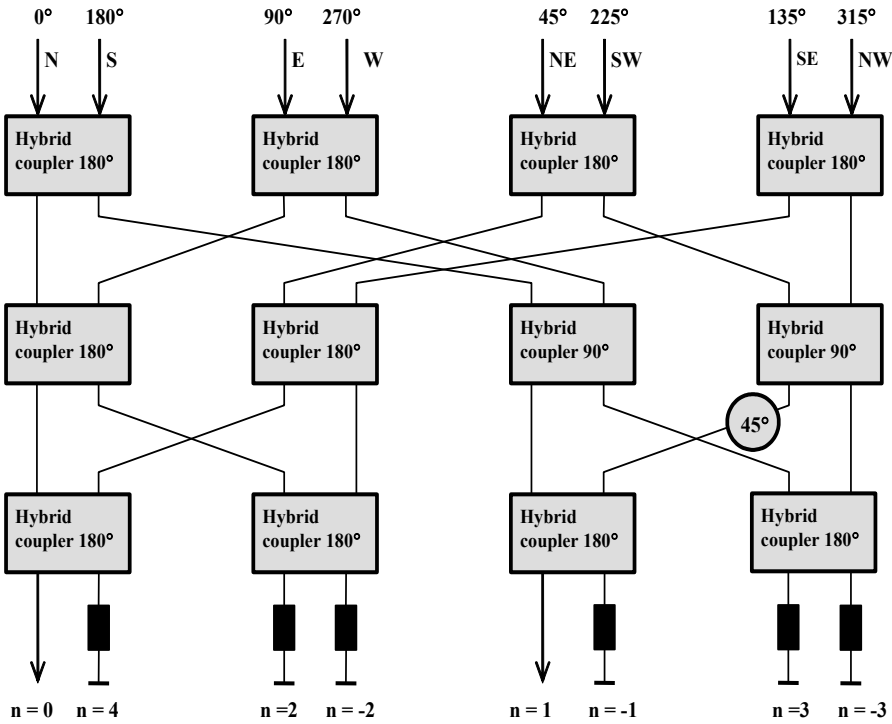


Fig. 3 The block diagram of the modified Butler matrix for feeding the interferometer bearing discriminator with eight antenna elements [2]

Tab. 3 Values of additional phase shifts of the MBM used for feeding the interferometer bearing discriminator with eight antennas [2]

Antenna (Sector)	DOA (Azimuth) [deg]	Additional Phase Shifts at MBM Output Ports [deg]								
		$n = 0$	$n = 1$	$n = -1$	$n = 2$	$n = -2$	$N = 3$	$n = -3$	$n = 4$	Δ $N = 1$ to 0
N	0	0	0	0	0	0	90	90	0	0
N-E	45	0	45	225	0	180	90	270	180	45
E	90	0	90	90	180	180	0	0	0	90
S-W	135	0	135	315	180	0 (360)	0	180	180	135
S	180	0	180	180	0	0	270	270	0	180
S-E	225	0	225	405 (45)	0	180	270	450 (90)	180	225
W	270	0	270	270	180	180	180	180	0	270
N-W	315	0	315	495 (135)	180	0 (360)	180	360 (0)	180	315

In the case of the MBM construction by means of real microwave circuits (i.e. hybrids and phase shifters) there is a basic disadvantage of the MBM design. The CAA design can only consist of the 2^N antenna elements.

Since the number of antenna elements does not have to be right equal to 2^N for practical PDFs, it is necessary to leave an approach or the physical MBM realisation and replace this MBM by its mathematical operation algorithm only as follows.

2.3. Mathematical Operation Algorithm of Modified Butler Matrix

To explain the MBM operation algorithm is unavoidable to design its mathematical model using of scattering matrices of hybrids including phase shifts of used phase shifters. The 2×2 MBM formed by hybrids only is illustrated in Fig. 4. The hybrids in the first line are the 180-degree hybrids and the next pair is made up by one 180-degree hybrid (HC₂₁) and one 90-degree hybrid (HC₂₂). For the description of input and output signals at the hybrid ports are used “a” letter (input signals) and “b” letter (output signals).

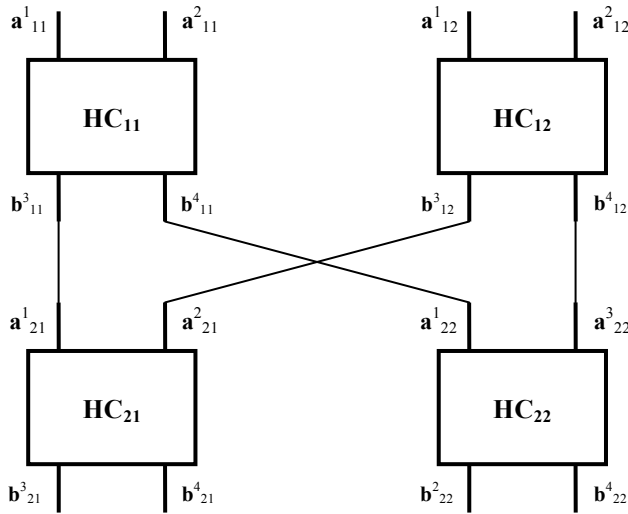


Fig. 4 The schematic illustration of input and output signals at MBM topology for operation algorithm derivation

The scattering matrix of the 180-degree hybrid is given by (1)

$$S_{180} = \frac{1}{\sqrt{2}} \begin{bmatrix} 0 & 0 & 1 & 1 \\ 0 & 0 & 1 & -1 \\ 1 & 1 & 0 & 0 \\ 1 & -1 & 0 & 0 \end{bmatrix}. \quad (1)$$

This matrix corresponds to the magic “T” circuit. The general scattering matrix of the 90-degree hybrid is expressed by (2a) and in case of the 3-dB divider it is possible to use (2b) as follows

$$s_{90} = \begin{bmatrix} 0 & \sqrt{1-p^2} & 0 & jp \\ \sqrt{1-p^2} & 0 & jp & 0 \\ 0 & jp & 0 & \sqrt{1-p^2} \\ jp & 0 & \sqrt{1-p^2} & 0 \end{bmatrix}, \quad (2a)$$

or

$$s_{90} = \frac{1}{\sqrt{2}} \begin{bmatrix} 0 & 1 & 0 & j \\ 1 & 0 & j & 0 \\ 0 & j & 0 & 1 \\ j & 0 & 1 & 0 \end{bmatrix}, \quad (2b)$$

when $p = \frac{1}{\sqrt{2}}$, resp. $\sqrt{1-p^2} = \frac{1}{\sqrt{2}}$.

Output signals at the 180-degree hybrid ports can be derived by (3)

$$\begin{bmatrix} b^1 \\ b^2 \\ b^3 \\ b^4 \end{bmatrix} = s_{180} \begin{bmatrix} a^1 \\ a^2 \\ a^3 \\ a^4 \end{bmatrix} = \frac{1}{\sqrt{2}} \begin{bmatrix} 0 & 0 & 1 & 1 \\ 0 & 0 & 1 & -1 \\ 1 & 1 & 0 & 0 \\ 1 & -1 & 0 & 0 \end{bmatrix} \begin{bmatrix} a^1 \\ a^2 \\ a^3 \\ a^4 \end{bmatrix}. \quad (3)$$

This equation can be used for output signal computing of any hybrid.

The output signal of the MBM output port $n=0$ corresponds to the signal designated as b_{21}^3 in Fig. 4. This signal is defined by (4a) when the input signal arrives from antenna ‘‘N’’ (a_{11}^1)

$$b_{21}^3 = \frac{\sqrt{2}}{2} a_{21}^1 = \frac{\sqrt{2}}{2} b_{11}^3 = \frac{\sqrt{2}}{2} \frac{\sqrt{2}}{2} a_{11}^1 = \frac{1}{2} a_{11}^1, \quad (4a)$$

The output signal at the MBM output port $n=0$ (b_{21}^3) is defined by (4b) when the input signal arrives from antenna ‘‘S’’ (a_{11}^2), etc.

$$b_{21}^3 = \frac{\sqrt{2}}{2} a_{21}^1 = \frac{\sqrt{2}}{2} b_{11}^3 = \frac{\sqrt{2}}{2} \frac{\sqrt{2}}{2} a_{11}^2 = \frac{1}{2} a_{11}^2, \quad (4b)$$

$$b_{21}^3 = \frac{\sqrt{2}}{2} a_{21}^2 = \frac{\sqrt{2}}{2} b_{12}^3 = \frac{\sqrt{2}}{2} \frac{\sqrt{2}}{2} a_{12}^1 = \frac{1}{2} a_{12}^1, \quad (4c)$$

$$b_{21}^3 = \frac{\sqrt{2}}{2} a_{21}^2 = \frac{\sqrt{2}}{2} b_{12}^3 = \frac{\sqrt{2}}{2} \frac{\sqrt{2}}{2} a_{12}^2 = \frac{1}{2} a_{12}^2. \quad (4d)$$

The output signal of the MBM output port $n=1$ corresponds to the signal designated as b_{22}^2 in Fig. 4. This signal is defined by (5a) when the input signal arrives from antenna ‘‘N’’ (a_{11}^1)

$$b_{22}^2 = s_{90} a_{22}^1 = \left(\frac{\sqrt{2}}{2} \ 1 \right) a_{22}^1 = \frac{\sqrt{2}}{2} b_{11}^4 = \frac{\sqrt{2}}{2} s_{180} a_{11}^1 = \frac{\sqrt{2}}{2} \left(\frac{\sqrt{2}}{2} \ 1 \right) a_{11}^1 = \frac{1}{2} a_{11}^1, \quad (5a)$$

The output signal at the MBM output port $n = 1$ (b_{22}^2) is defined by (5b) when the input signal arrives from antenna “S” (a_{11}^2), etc.

$$b_{22}^2 = s_{90} a_{22}^1 = \left(\frac{\sqrt{2}}{2} 1\right) a_{22}^1 = \frac{\sqrt{2}}{2} b_{11}^4 = \frac{\sqrt{2}}{2} s_{180} a_{11}^2 = \frac{\sqrt{2}}{2} \left(\frac{\sqrt{2}}{2} (-1)\right) a_{11}^2 = \frac{1}{2} a_{11}^2 e^{j\pi}, \quad (5b)$$

$$b_{22}^2 = s_{90} a_{22}^3 = \left(\frac{\sqrt{2}}{2} j\right) a_{22}^3 = \frac{\sqrt{2}}{2} j b_{11}^4 = \frac{\sqrt{2}}{2} j s_{180} a_{12}^1 = \frac{\sqrt{2}}{2} j \left(\frac{\sqrt{2}}{2} 1\right) a_{12}^1 = \frac{1}{2} a_{12}^2 e^{j\frac{\pi}{2}}, \quad (5c)$$

$$b_{22}^2 = s_{90} a_{22}^3 = \left(\frac{\sqrt{2}}{2} j\right) a_{22}^3 = \frac{\sqrt{2}}{2} j b_{11}^4 = \frac{\sqrt{2}}{2} j s_{180} a_{12}^2 = \frac{\sqrt{2}}{2} j \left(\frac{\sqrt{2}}{2} (-1)\right) a_{12}^2 = \frac{1}{2} a_{12}^2 e^{j\frac{3\pi}{2}}. \quad (5d)$$

The detailed insight of results obtained from (5a) to (5d) shows that signals at the MBM output port $n = 1$ from the particular antenna elements of the CAA can be seen as vectors in the complex plane. The magnitude of each vector is given by the amplitude of the intercepted signal and the argument of this vector is equal to the direction angle of the antenna element boresight, i.e. the antenna “N” gives the argument in the form e^{j0} , the antenna “E” gives $e^{j\frac{\pi}{2}}$, etc.

In the DOA determination case of an intercepted signal it is essential to use all signals captured by the CAA elements. The sum of these output signals (virtually vectors) defines the resulting signal vector and its argument determines the required DOA of the signal source.

The required resulting vector for the four-element CAA used for omnidirectional interception of signals of interest in the azimuth plane is provided by (6) (i.e. for the whole interval 0 to 360 degrees of the azimuth)

$$b_{22}^2 = \frac{1}{2} \left[a_{11}^1 e^{j0} + a_{12}^1 e^{j\frac{\pi}{2}} + a_{11}^2 e^{j\pi} + a_{12}^2 e^{j\frac{3\pi}{2}} \right]. \quad (6)$$

In practice, it is more convenient to express the intercepted signal amplitude by means of an antenna gain of the relevant antenna elements whereas the value of this antenna gain is affected by the direction which the incoming signal arrives from. Therefore the other notation can be used and (6) can be rewritten as follows:

$$OUT(\mathcal{G}) = \frac{1}{2} \left(IN_1 e^{j0} + IN_2 e^{j\frac{\pi}{2}} + IN_3 e^{j\pi} + IN_4 e^{j\frac{3\pi}{2}} \right), \quad (7)$$

where $OUT(\mathcal{G})$ is a signal at the MBM output port $n = 1$ (likewise a vector in the complex plane) for the DOA – the azimuth \mathcal{G} ,

IN_i is the signal at the MBM input port, the index $i = 1 \div N$, when N is equal to 4 in the case of the four-element CAA,

and

$$IN_i = G_i(\mathcal{G}),$$

where $G_i(\mathcal{G})$ is the antenna pattern gain of the i -th CAA antenna element at the direction \mathcal{G} (azimuth) which the signal of interest is arriving from.

For the four-element CAA ($N = 4$), the expression (7) can be rearranged if the antenna element spacing is constant and the spatial angle between the adjacent antenna

boresight is equal to 90 degrees, or $\pi/2$ radians, respectively. In this case, it is possible to obtain (8)

$$OUT(\vartheta) = \frac{1}{2} \sum_{i=1}^N G_i(\vartheta) e^{j(i-1)\frac{\pi}{2}}. \quad (8)$$

If the CAA uses an arbitrary number of antenna elements for the omnidirectional interception of signals, the term (8) is rewritten to the form (9) as follows:

$$OUT(\vartheta) = \frac{1}{2} \sum_{i=1}^N G_i(\vartheta) e^{j\frac{2\pi}{N}(i-1)}. \quad (9)$$

The basic condition for using the above mentioned equation is the equiangular spacing between adjacent boresights of used antenna elements that cover the whole azimuth plane (i.e., 360 degrees, or 2π radians, respectively) by their antenna patterns. Thus, this expression is the common mathematical expression that can be used for any omnidirectional multi-lobe PDF satisfying the defined condition [5].

For the DOA determination of the signal intercepted by relevant CAA elements it is possible to use (10) that defines the value of the resulting complex vector argument, i.e. the required azimuth angle of the signal of interest

$$DOA = \tan^{-1} \left(\frac{\text{Im}\{OUT(\vartheta)\}}{\text{Re}\{OUT(\vartheta)\}} \right). \quad (10)$$

This resultant expression can be implemented to signal processing circuits of the omnidirectional multi-lobe PDF and it enables to perform the DOA determination task by the digital way [5].

3. Passive Direction Finder Design with Circular Antenna Array Using of MBM Operation Algorithm

The system design of the omnidirectional multi-lobe PDF with the N -element CAA in the form of the schematic block diagram is shown in Fig. 5. This concept of the PDF supposes that the designed equipment can use an arbitrary number of antenna elements and consequently the MBM operation algorithm for the DOA determination of intercepted signals. Therefore the relevant MBM will not be used for interconnecting the CAA elements and the signal processing circuits that will be used for the DOA determination by means of the digital DF methods with the mathematical calculation derived above.

The number N of the used antenna elements depends mainly on the required accuracy of the signal DOA determination and the antenna pattern parameters (e.g. directive features) of these antenna elements. It means that the directivity of the used antennas will affect the adequate signal-to-noise ratio (SNR) and the number of input signals included to the calculation of the signal DOA determination.

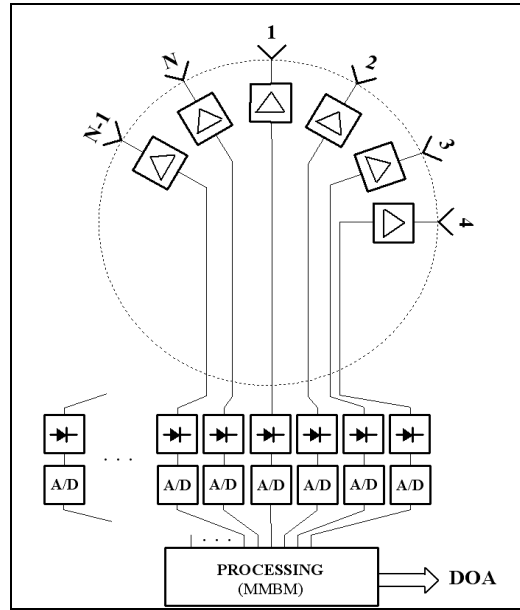


Fig. 5 Basic block diagram of the multi-lobe passive digital direction finder [2]

For the required power level of intercepted signals at the antenna element outputs, RF amplifiers follow the antenna elements in the block diagram of the PDF. The RF amplifier outputs are led to the microwave detectors that give magnitudes of the detected signal amplitudes. To obtain the digital form of received signal magnitude, analogue-to-digital (A/D) converters are used. Their outputs are connected to the signal processing circuits. The result of this digital signal processing (DSP) then is the DOA determination of received signals intercepted by the CAA of the designed omnidirectional multi-lobe PDF.

From the correct DOA determination point of view it is necessary to ensure the linear signal processing realised by the DSP circuits. This linearization will reduce an influence of an incorrect antenna pattern shape of the used CAA elements, an amplification of the used RF amplifiers, and a detection of the used microwave detectors in consequence of non-linear operation characteristics of these microwave elements.

4. DOA Determination by means of Passive Direction Finder – Experimental Measuring and Results

The results presented in the previous parts imply that the used antenna elements of the CAA have the most important role in the omnidirectional multi-lobe PDF design. To evaluate the introduced design of the PDF concept in practice, an experimental CAA was used. The experimental CAA consisted of several hog-horn antennas designed for X-band and the photograph of this CAA with six hog-horns is shown in Fig. 6.

The experimental CAA enables to change the number of antenna elements used for the signal DOA determination, their mutual position, and the spacing between the boresights of the adjacent antennas.

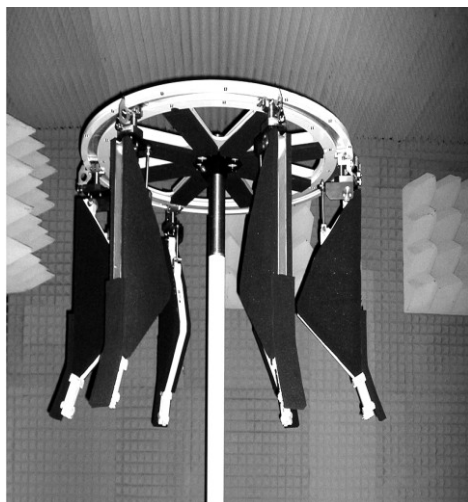


Fig. 6 Photograph of experimental CAA with six hog-horn antennas of X-band

The error magnitude of the signal DOA determination was chosen as a criterion for evaluating the correct results of the PDF operation. This error was defined as a difference between the known DOA value of the emitter whose signal was intercepted by the used CAA, and the signal DOA value determined by means of the digital DF method for given real antenna patterns of the CAA elements or an approximation of the antenna pattern by the appropriate analytic curve when the best approximation of the real hog-horn antenna pattern was reached by using of the Gaussian curve.

4.1. DOA Determination by Means of Six-element Multi-lobe Passive Direction Finder with MBM Operation Algorithm Using

To evaluate possibilities of the designed PDF with six-element CAA (the equiangular spacing among antenna elements is 60 degrees), there was designed and applied a mathematical model of the omnidirectional multi-lobe PDF that used the real antenna pattern approximation by the relevant Gaussian curve. The corresponding antenna pattern of this mathematical model is shown in Fig. 7.

Fig. 8 represents interpolated values of the output power magnitude of signals intercepted by the six-element CAA at the microwave detector outputs for the whole interval of azimuth angles from 0 to 360 degrees. These output power values were used for the signal DOA determination by means of the digital DF methods and the obtained results of the DOA determination were compared with the results of mathematical simulation of the omnidirectional multi-lobe PDF operation.

Fig. 9 shows the signal DOA determination results obtained by the comparison of measured signal amplitude values and the mathematical PDF operation simulation. Waveforms express error magnitudes of the DOA determination at relevant azimuth angles for real measured signals intercepted by the hog-horn antennas (*solid line*) compared to the mathematical simulation results in the same azimuths (*criss-cross line*).

To determine the signal DOA by means of the digital DF method, only the two strongest signals were always used. The both presented curves of the DOA determination error show the very good measure of the resulting error coincidence at

the given azimuth (the DOA). Possible differences are caused by the inaccuracy of the real signal amplitude magnitude measuring.

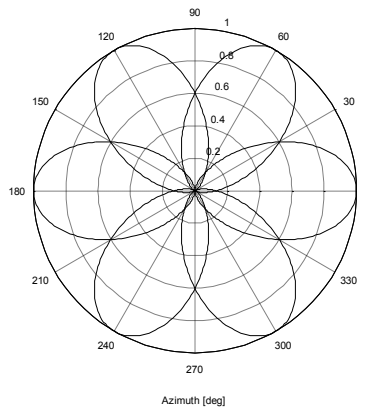


Fig. 7 Ideal antenna pattern of six-element CAA approximated by Gaussian curves (in polar coordinates)

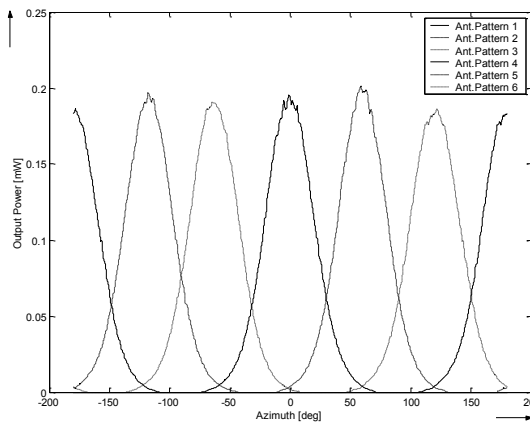


Fig. 8 Measured power magnitudes of output signals intercepted by the six-lobe passive DF system

Waveforms in Fig. 10 have the same meaning as the results presented in Fig. 9. The difference consists only in the number of used signals for the DOA determination. Fig. 10 presents the values of the signal DOA determination error for the three strongest intercepted signals used for the DOA calculation. A certain discrepancy between the real data and the mathematical simulation results is again caused by the inaccuracy of the real signal amplitude magnitude measuring.

The figures show that the error values of the signal DOA determination decrease with the growing number of intercepted signals used for the signal DOA calculation. The least errors of the signal DOA determination belonged to azimuths where the antenna patterns of the adjacent elements crossed. However, in the case of the six-element CAA, further increase of the signal number is not possible because the

antenna pattern of the hog-horn antenna is not wide enough ($\Theta_{-3dB} \cong 50$ degrees) and subsequent intercepted signals are not available.

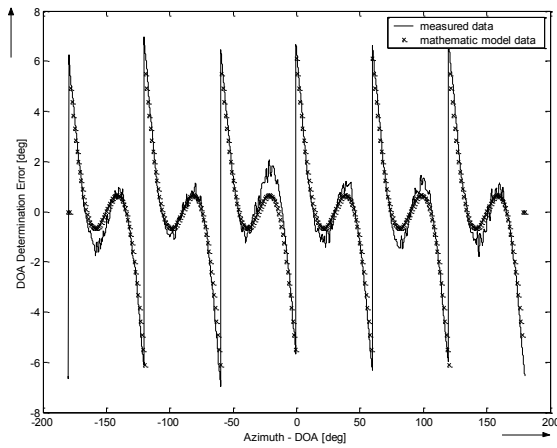


Fig. 9 DOA determination error values for the two strongest signals used for DOA computing (six-element CAA)

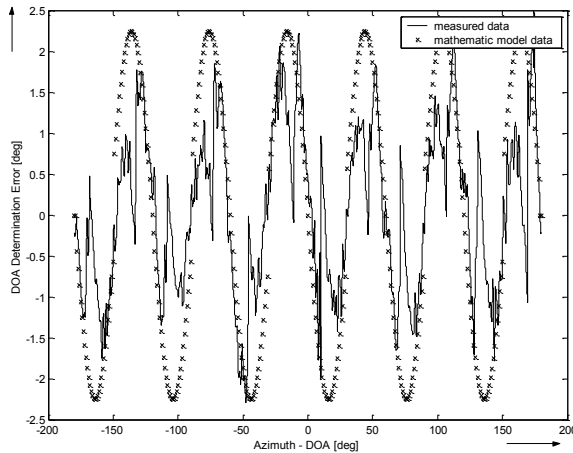


Fig. 10 DOA determination error values for the three strongest signals used for DOA computing (six-element CAA)

4.2. DOA Determination by Means of Eight-element Multi-lobe Passive Direction Finder with MBM Operation Algorithm Using

For better evaluation of the antenna element number influence on the signal DOA determination, the results for the eight-element CAA of the PDF are presented. This means the equiangular spacing among antenna elements is 45 degrees. For this example of the CAA, the procedure of the signal DOA determination and an evaluation of obtained results were made in the same way as in the case of the six-element CAA and the corresponding PDF mathematical model.

Figs 11 and 12 show the signal DOA determination results by the comparison of measured signal amplitude values and the mathematical PDF operation simulation for the eight-element CAA. Waveforms again express the error magnitudes of the DOA determination at the relevant azimuth angle for real measured signals intercepted by used hog-horn antennas (*solid line*) compared to the mathematical simulation results in the same azimuths (*criss-cross line*).

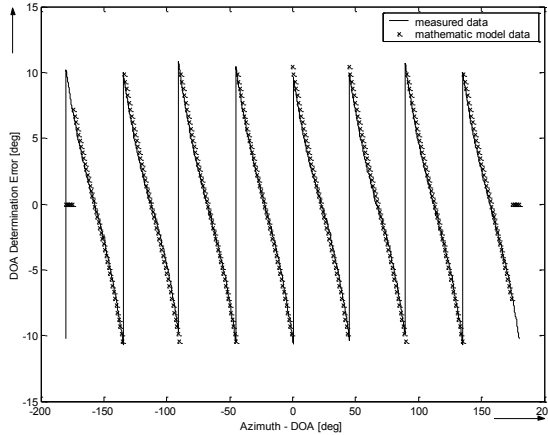


Fig. 11 DOA determination error values for the two strongest signals used for DOA computing (eight-element CAA)

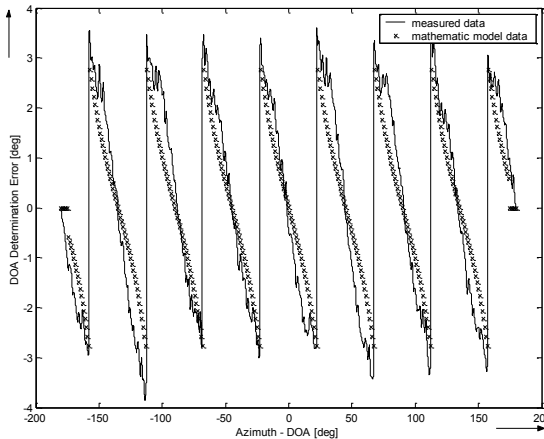


Fig. 12 DOA determination error values for the three strongest signals used for DOA computing (eight-element CAA)

The comparison of the DOA determination error results presented in Fig. 9 vs. Fig. 11 and the results presented in Fig. 10 vs. Fig. 12 shows that the six-element CAA reaches less error values of the signal DOA determination than the eight-element CAA. This conclusion results first of all from using of the hog-horn antennas that has the 3-dB beamwidth approximately 50 degrees, or less. Therefore the better results were obtained for six-element than the eight-element CAA. The detailed analysis and

evaluation of the influence of an antenna pattern shape as well as an antenna element number on the DOA determination error values are introduced in [6].

5. Conclusion

The introduced concept of the omnidirectional multi-lobe PDF with the MBM operation algorithm using for the signal DOA determination enables to find out the required signal DOA for any azimuth unambiguously and with sufficient accuracy. This signal DOA determination accomplished by the above derived digital amplitude DF method is realised on the basis of the knowledge of the intercepted signal amplitude magnitude and the corresponding antenna element boresight value only.

In contrast to the majority of known and often used comparative DF method, the introduced digital DF method enables to use the major number of intercepted signals (i.e. more than 2) for improving the DOA determination accuracy with respect to directive characteristics of used antenna elements. Simultaneously, the use of an arbitrary number of antenna elements for covering the whole azimuth plane is given just with respect to directive characteristics of the CAA elements and the required SNR at the antenna element outputs.

References

- [1] HOSKO, E. and VESELY, J. The Direction of Arrival Acquisition via the Modified Butler Matrix Signal Processing, In *Proceedings of International Conference Applied Electronics 2002*. Plzeň (CZ) : University of West Bohemia, 2002, p. 79-83. ISBN 80-7082-881-1.
- [2] HOSKO, E. and ZEMAN, M. Digital Method of Signal Direction Finding via Multi-beam Circular Antenna Array, In *Proceedings of International Conference on Military Technologies ICMT'07*. Brno (CZ) : University of Defence, 2007, p. 366-376. ISBN 978-80-7231-238-2.
- [3] FOURIKIS, N. *Phased Array-Based Systems and Applications*. New York : Wiley, 1997. ISBN 0-471-01212-2.
- [4] LIPSKY, S. E. *Microwave Passive Direction Finding*. New York : Wiley, 1988. ISBN 0-471-83454-8.
- [5] HOSKO, E. and VESELY, J. ELINT/ESM Direction Finding System with Multi-lobe Antenna Array and its Possibilities as Passive Sensor for Network Enabling Capabilities, In *Proceedings of a conference MCC'07*, Bonn (Germany) : Forschungsgesellschaft für Angewandte Naturwissenschaften, 2007. 9 p. ISBN 978-3-934401-16-7.
- [6] HOSKO, E. *Direction of Arrival Determination via Circular Antenna Array for Passive Direction Finding System of Target Tracking* (in Czech) [Research Report]. Brno (CZ) : University of Defence, 2009. 129 p.

Acknowledgement

The work presented in this paper has been supported by the Ministry of Defence of the Czech Republic (research project No. MO0FVT0000402).